



<b>Title</b>	<b>Phase modulator defined by impurities induced disordering</b>
<b>Author(s)</b>	<b>Lo, KM; Choy, WCH; Li, EH</b>
<b>Citation</b>	<b>Materials Research Society Symposium - Proceedings, 1997, v. 450, p. 383-388</b>
<b>Issued Date</b>	<b>1997</b>
<b>URL</b>	<b><a href="http://hdl.handle.net/10722/46028">http://hdl.handle.net/10722/46028</a></b>
<b>Rights</b>	<b>Creative Commons: Attribution 3.0 Hong Kong License</b>

## PHASE MODULATOR DEFINED BY IMPURITIES INDUCED DISORDERING

K. M. Lo\*, W. C. H. Choy\*\*, E. H. Li\*\*\*

\* Quincy, MA

\*\* Department of Electronic and Electrical Engineering, University of Surrey, U.K.

\*\*\* Department of Electrical and Electronic Engineering, University of Hong Kong, H.K.

### ABSTRACT

Optical waveguide type phase modulators defined by impurities induced disordering (IID) are investigated. To achieve a better optical confinement, a two steps ion implantation process is carried out to introduce additional impurities with respect to depth in the cladding region. A more uniform refractive index profile in deeper lateral confined region is obtained after thermal annealing. The refractive index different between the core and cladding can be adjusted by controlling the extension of interdiffusion in the cladding. This provide tuning of single mode operating region. For present IID phase modulator with 25 period of  $100\text{\AA}/100\text{\AA}$   $\text{Al}_{0.3}\text{Ga}_{0.7}\text{As}/\text{GaAs}$  multiple quantum wells single mode operating at  $0.88\mu\text{m}$ , a normalized phase shift of  $362^\circ/\text{Vmm}$ , chirping parameter of 47, and absorption loss less than  $120\text{cm}^{-1}$  are achieved theoretically.

### INTRODUCTION

Different III-V semiconductor quantum wells (QWs) materials have been intensely investigated in electro-optical phase modulator [1, 2]. The use of QWs material has an advantage of large variation in the electric field induced refractive index change due to the quantum confined Stark effect in the QW around the excitonic absorption edge as compared to those in conventional materials like bulk III-V semiconductors and  $\text{LiNbO}_3$ . However, most of the QW phase modulator are single insulated component [1, 2]. In order to obtain an efficient way of monolithic integration of optoelectronics components on a single substrate, a technique of impurities induced disordering has been utilized to integrate optoelectronics [3, 4]. Impurities are introduced selectively by masked implantation followed by diffusion into the desired regions of a QW structure, a modification of the bandgap and a refractive index step would be result between the as-grown and the disordered regions [5]. The IID process therefore enables a planar process to be used to fabricate and insulate different optical devices such as laser [6], modulator [7] and waveguide [8] on single substrate and makes optoelectronic integration a reality.

A theoretical model is developed to investigate IID lateral confined  $\text{AlGaAs}/\text{GaAs}$  QW phase modulators. The modulators are single mode operation. To increase optical confinement and phase modulation, twice ion implantation with different implantation energies are introduced. The model of IID by ion implantation, optical guiding and modulation properties will be given in the next section. In the third section, results on single mode phase modulation and modulation performance will be presented.

## COMPUTATION CONSIDERATIONS

### Impurities Induced Disorder by Ion Implantation

For present phase modulator, the active region consists of stacked  $\text{Al}_{0.3}\text{Ga}_{0.7}\text{As}/\text{GaAs}$  as-grown QWs. With a core region presisted by a mask, two lateral regions of the QWs are ion-implanted by Ga ions for cladding. After thermal annealing, the QWs structure with the implanted impurities has lower refractive index than the intrinsic region, hence provide a lateral optical confinement to the active cavity.

The impurity density is computed in a two dimensional structure. The distribution of impurities after implantation  $W(x, y)$ , where  $x$  and  $y$  is defined as the lateral direction and depth of the structure respectively, is described by an error function relation based on the experimental and simulation results [10]. The total impurities distribution  $W_T(x, y)$  is obtained by linear summation of each, i.e.

$$W_T(x, y) = \sum_{i=0}^M W_i(x, y), \quad (1)$$

where  $W_i(x, y)$  is the  $i$ -th impurities profile of the total  $M$  times of implantation. A classical diffusion law is used to described the the motion of the impurities during annealing time  $t$

$$\frac{\partial W_T(x, y, t)}{\partial t} = D_{\text{ion}} \nabla^2 W_T(x, y, t). \quad (2)$$

For short annealing time, the diffusion of impurities is assumed to be independent of the motion of Al/Ga atoms and the diffusion coefficient  $D_{\text{ion}}$  is a constant through out the annealing. Moreover, the interdiffusion coefficient of Al/Ga,  $D_{\text{atom}}$ , is assumed to be depend on local defect density only, i.e.  $D_{\text{atom}}(x, y, t) = \alpha D_{\text{ion}}(x, y, t)$ .  $\alpha$  is a numerical factor determined from experimental data. The diffusion equation for Al/Ga atoms is given by

$$\frac{\partial C(x, y, t)}{\partial t} = \nabla [D_{\text{atom}} \nabla C(x, y, t)], \quad (3)$$

where  $C(x, y, t)$  is the Al/Ga concentration. Solving (3), the Al/Ga concentration profile can be obtained from which its corresponding diffusion length  $L_d$  [11] is determined. Using a developed model [11], a refractive index profile  $n(x, y)$  is calculated for different  $L_d$ .

### Scalar Wave Equation

Given the refractive index profile of IID phase modulator, its optical guiding properties are studied by means of solving the scalar wave equation

$$\left[ \frac{\partial^2}{\partial x^2} + \frac{\partial^2}{\partial y^2} + k^2 n^2(x, y) - \beta^2 \right] \Psi(x, y) = 0, \quad (4)$$

where  $\Psi(x, y)$  denotes the transverse modal electric field,  $k = 2\pi/\lambda$ , where  $\lambda$  represents the free-space wavelength and  $\beta$  is the associated propagation constant. (4) is solved by an improved Fourier decomposition method [13].

The modulation performance of the phase modulator is interpreted in terms of several measuring parameters. The first one is modulation efficiency of the phase modulation which can be measured from the phase change per modulation length and applied voltage or in normalized phase shift as  $\Delta\theta_N = 2\pi\Delta n_{\text{eff}}/(V\lambda_{\text{op}})$ , where  $\Delta n_{\text{eff}} = \Delta\beta/k$  is change of effective refractive index,  $\lambda_{\text{op}}$  is the operating wavelength and  $V$  is the applied voltage which is calculated by the Poisson's equation [12]. For present phase modulator, the selected  $\lambda_{\text{op}}$  (in eV) is less than the bandgap energy of the  $\text{Al}_{0.3}\text{Ga}_{0.7}\text{As}/\text{GaAs}$  cladding layers. Therefore, it is assumed that only the optical power confined in the active cavity will be absorbed. Since the active cavity is constructed from QWs material, the optical confinement factor  $\Gamma$  can be defined as the ratio of optical electric field in QWs (active cavity) and the whole structure.

The effective absorption coefficient is given by  $\alpha_{\text{eff}} = \int_{\text{QWs}} \alpha(x, y)\Psi^2 dA / \int_{\infty} \Psi^2 dA$ , where  $\alpha(x, y)$  is material absorption coefficient of the  $\text{Al}_{0.3}\text{Ga}_{0.7}\text{As}/\text{GaAs}$  QWs structure. Under non-bias condition,  $\alpha_{\text{eff}}$  is considered as the absorption loss of the modulator.

The chirping parameter is a crucial indicator to the performance of the modulator. Under bias, both  $n_{\text{eff}}$  and  $\alpha_{\text{eff}}$  will change, the static chirping parameter  $\beta_{\text{mod}}$  is given as  $\beta_{\text{mod}} = 4\pi\Delta n_{\text{eff}}/(\lambda_{\text{op}}\Delta\alpha_{\text{eff}})$ , where  $\Delta\alpha_{\text{eff}}$  is the change of effective absorption. From this relation,  $\beta_{\text{mod}}$  can be considered as a measure of the relative strength of the phase modulation to that of intensity modulation. To be a good phase modulator, the chirping parameter should greater than 10 [14].

## RESULTS AND DISCUSSIONS

The active region of the proposed IID electro-optical phase modulator consists of multiple periods of  $100\text{\AA}/100\text{\AA}$   $\text{Al}_{0.3}\text{Ga}_{0.7}\text{As}/\text{GaAs}$  as-grown QWs. Results of two active cavity of  $0.5\mu\text{m}$  thick (25 QW periods) and  $1\mu\text{m}$  thick (50 QW periods) are presented in this section. The top and bottom layer of the modulator are heavily p and n doped  $\text{Al}_{0.3}\text{Ga}_{0.7}\text{As}$  to form a p-i-n structure. The whole device is fabricated on a  $n^+$ -GaAs substrate. The modulation under applied field  $F$  of  $50\text{kV}/\text{cm}$  and  $100\text{kV}/\text{cm}$  are studied at  $\lambda_{\text{op}}$  of  $0.88\mu\text{m}$ .

A typical refractive index profile after single step of ion implantation is shown in Fig. 1(a). The modification of the refractive index near the top and bottom of the ion implanted cladding layer is small such that optical power leaks out from these regions as shown in Fig. 1(b) and weakening the guiding property. In order to improve the optical confinement, ion implantation is carried out twice, one with shallower and one with deeper penetration depth to produce a combined impurities distribution with greater uniformity in the depth of the cladding layer. By carefully adjusting the implantation energies, the region with uniform refractive index clearly extends as shown in Fig. 2(a). Optical field profile of the corresponding guiding mode is shown in Fig. 2(b). The guiding property of this twice ion-implanted structure improves as comparing with field profile of the one step ion-implanted structure in Fig. 1(b).

The ion-implanted diffusion is carefully designed to adjust the refractive index for single mode operation. Present results shown that a range of material refractive index profile can serve for single modal modulation at the selected  $\lambda_{\text{op}}$  of  $0.88\mu\text{m}$ . This is illustrated by plotting the normalized propagation constant  $b = ((\beta/k)^2 - n_{\text{min}}^2)/(n_{\text{max}}^2 - n_{\text{min}}^2)$ , where  $n_{\text{max}}$  and  $n_{\text{min}}$  are the maximum and minimum refractive index of the active cavity, against annealing time  $t$  (which stands for the refractive index profile) as shown in Fig. 3.

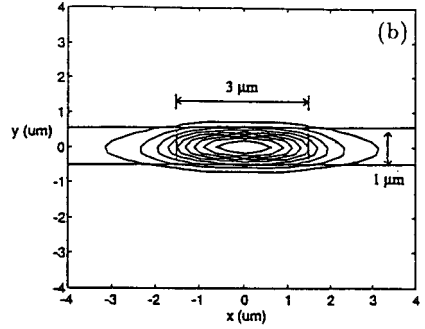
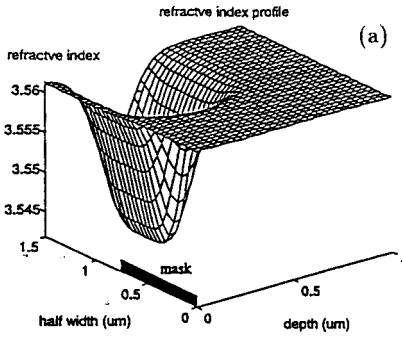


Figure 1: (a) The refractive index profile of half cross-section device structure provided by one ion implantation. (b) Contour of optical field of the corresponding guiding mode.

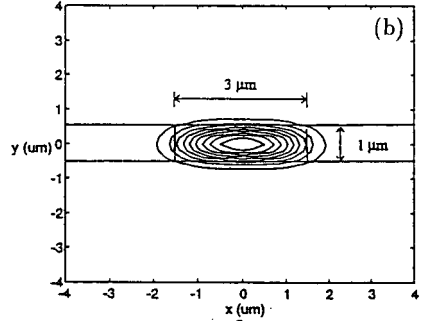
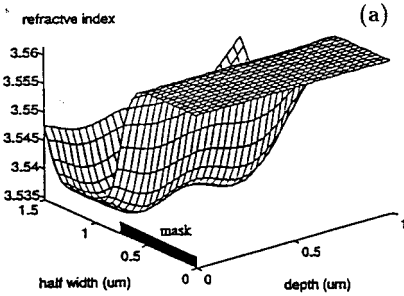


Figure 2: (a) The refractive index profile of half cross-section device structure provided by twice ion implantation. (b) Contour of optical field of the corresponding guiding mode.

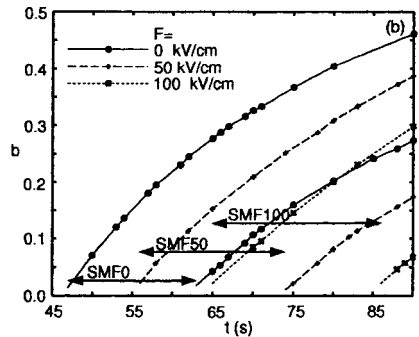
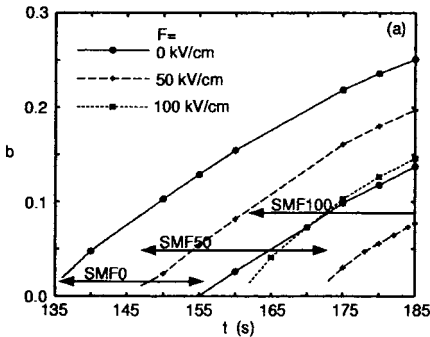


Figure 3: Normalized propagation constant  $b$  against annealing time  $t$  for cavity thickness of (a)  $0.5\mu\text{m}$  and (b)  $1.0\mu\text{m}$ . Annealing time is shorter for fundamental mode .

Table 1: Modulation parameters of two phase modulators with cavity thickness of  $0.5\mu\text{m}$  (25 QW periods) and  $1\mu\text{m}$  (50 QW periods).

Thickness ( $\mu\text{m}$ )	0.5		1	
bias field (kV/cm)	0	50	0	50
bias voltage (V)	0	2.54	0	5.04
$\Gamma$	0.843	0.839	0.919	0.911
$n_{\text{eff}}$	3.5138	3.5116	3.5421	3.540
$\Delta n_{\text{eff}}$	-	$-2.22 \times 10^{-3}$	-	$-2.40 \times 10^{-3}$
depletion width ( $\mu\text{m}$ )	-	0.507	-	1.01
$\Delta\theta_N$ ( $^\circ/\text{Vmm}$ )	-	362	-	194
$\alpha_{\text{eff}}$ ( $\text{cm}^{-1}$ )	117.3	110.7	132	123.6
$\Delta\alpha_{\text{eff}}$ ( $\text{cm}^{-1}$ )	-	-6.6	-	-8.4
$\beta_{\text{mod}}$	-	+47	-	+41

The intervals SMF0, SMF50 and SMF100 corresponds to single mode operation under field strength of 0, 50 and 100kV/cm. With an applied field, the refractive index profile, and thus the propagation mode, is modified. The interval therefore modifies as shown in Fig. 3. The waveguide modulator may support single mode or multiple mode guiding at the selected  $\lambda_{\text{op}}$ . In order to maintain single mode operation, only the overlapping region between two intervals with different applied fields, such as the overlapping region between SMF0 and SMF50 of Fig. 3, can provide a single mode phase modulation. In fact, the modulation can also work between SMF50 and SMF100 which provide a much larger overlapping range for operation. However, there must have some resistance loading in an electrical circuit for electro-optical modulation, in order to reduce the power consumption of the phase modulation, the one without bias requirement is selected, i.e. the case without a d.c. offset. Between SMF0 and SMF100, there are no overlapping meaning that single modal phase modulation up to a bias field of 100kV/cm does not exist. In fact, present phase modulator can provide a large enough modulation between 0 and 50kV/cm.

The performance of the two modulators is listed in Table 1. The normalized phase shifts  $\Delta\theta_N$  are large enough that over  $180^\circ$  phase modulation can be obtained. For the  $0.5\mu\text{m}$  thick cavity, a two fold increase of  $\Delta\theta_N$  is seen when compared with  $1\mu\text{m}$  thick cavity while maintain a low absorption loss of less than  $150\text{cm}^{-1}$ . This shows that applied field of 50kV/cm is large enough to bias the modulator with an useful phase modulation. For the  $1\mu\text{m}$  thick cavity, its phase modulation under 50kV/cm is larger than that of  $0.5\mu\text{m}$  one since the optical confinement increase in the thicker cavity and also in which twice number of QWs contribute for modulation. However, its active thickness is two times of the thinner structure meaning that twice bias voltage is required for the same amount of applied field. This results in a weaker normalized phase shift. The  $\beta_{\text{mod}}$  obtained indicates that the phase modulation is at least 40 times greater than the intensity modulation at the selected  $\lambda_{\text{op}}$ , this is four fold large than the basic requirement of phase modulator. Under the 50kV/cm applied field, the depleted thickness of both cases are thicker than their corresponding cavity thickness and hence, during operation, the QWs structures produced for phase modulation are completely and effectively used.

## CONCLUSION

Optical waveguide type phase modulators with  $0.5\mu\text{m}$  and  $1\mu\text{m}$  thick QWs active cavity using masked ion-implantation to selective induce disordering to the QWs have been investigated. These devices are carefully designed to achieve single mode operation at  $0.88\mu\text{m}$ . For the  $1\mu\text{m}$  thick cavity, twice ion implantation is introduced to provide a wider cladding region with uniform refractive index. This improve the optical confinement and hence the phase modulation under same amount of bias as compared to the  $0.5\mu\text{m}$  one. However, in terms of the normalized phase shift and power consumption, thin cavity provide better modulation performance. In summary, the two phase modulators can provide large phase change, normalized phase shift of  $362^\circ/\text{Vmm}$  and  $194^\circ/\text{Vmm}$  for the  $0.5\mu\text{m}$  and  $1\mu\text{m}$  thick cavity respectively. Chirping parameter of more than 40 with frequency compression property is achieved and absorption loss is less than  $150\text{cm}^{-1}$ . This make present phase modulator become a competitive among the QW phase modulation devices.

## ACKNOWLEDGEMENTS

The authors would like to thank the University of Hong Kong, Committee on Research and Conference (CRGC) for financial support. Wallace C. H. Choy would like to express his warmest gratitude for the financial support of the Sir Edward Youde Fellowship.

## REFERENCES

1. S. Yoshida, Y. Tada, I. Kotaka, and K. Wakita, *Electron. Lett.* **30**, 1795 (1994).
2. H.K. Tsang, J.B.D. Soole, H.P. Le Blane, R. Bhat, M.A. Koza, and I.H. White, *Appl. Phys. Lett.* **57**, 2285 (1990).
3. S.R. Andrew, J.H. Marsh, M.C. Holland, and A.H. Kcan, *IEEE Photon. Technol. Lett.* **4**, 426 (1992).
4. T. Miyazawa, H. Iwamura, and M. Naganuma, *IEEE Photon. Technol. Lett.* **3**, 421 (1991).
5. C. Vien, M. Schneider, D. Mailly, R. Planel, H. Launois, H.Y. Marzin and B. Descouts, *J. Appl. Phys.* **70**, 1444 (1991).
6. P.J. Poole, S. Charbonnesu, M. Dion, G.C. Aers, M. Buchana, R.D. Golderb, and I.V. Mitchell, *IEEE Photon. Technol. Lett.* **8**, 16 (1996).
7. D.G. Deppe, L.H. Guido, M. Holonyak Jr., K.C. Hsieh, R.D. Burnham, D.L. Thornton and E.L. Paoli, *Appl. Phys. Lett.* **49**, 510 (1986).
8. E. Kapon, N.G. Stoffel, E.A. Dobisz, and R. Bhat, *Appl. Phys. Lett.* **52**, 351 (1988).
9. P. J. Bradley and G. Parry, *Electron. Lett.* **25**, 1349 (1989).
10. D. Briggs and M. P. Seah, Eds., *Ion and Neutral Spectroscopy*, vol. 2 of *Practical Surface Analysis*, Wiley, Chicheater, 2nd (1992).
11. E.H. Li, B.L. Weiss, K.S. Chan, and J. Micallef, *App. Phys. Lett.* **62**, 550 (1993).
12. W.C.H. Choy, and E.H. Li, *IEEE J. of Quantum Electron.*, to be appeared.
13. S. J. Hewlett, and F. Ladouceur, *J. Lightwave Technol.* **13**, 375 (1995).
14. T. Hausken, R. H. Yan, R. I. Simes, and L. A. Coldren, *Appl. Phys.* **55**, 718 (1989).